Optical Materials

DOI: 10.1002/anie.200904156

Efficient and Stable Blue Electrogenerated Chemiluminescence of Fluorene-Substituted Aromatic Hydrocarbons**

Khalid M. Omer, Sung-Yu Ku, Ken-Tsung Wong, and Allen J. Bard**

Tailored molecular structure is the key to tune the electronic and spectroscopic properties of a molecule. This is always a goal in electrogenerated chemiluminescence (ECL), that is, to have a material with high photoluminescence (PL) quantum yield and stable, long-lived radical ions in solution upon oxidation and reduction. Among various ECL active materials, polyaromatic hydrocarbons (PAHs) were the earliest subjects of ECL studies,[1] and substituted PAHs have been widely investigated.[2] Indeed, the PAHs 9,10-diphenylanthracene (DPA) and rubrene (R) have usually been used as ECL standards.[1a] These molecules are intense ECL emitters because of their high fluorescence quantum yields and stable radical cations and anions in aprotic media. However, the ECL emission of DPA and R eventually decays. This might be attributed to the irreversibility of the second oxidation because of the instability of the dication, for example, DPA^{2+}. Although for generation of ECL spectra, the radical ions are typically obtained by pulsing the electrode potentials, slightly beyond (≈ 100 mV) the first reduction and oxidation peak potentials, there is always some disproportionation of the radical cation leading to dication production. Thus, instability of doubly charged ions leads to slow decomposition. If the second oxidation wave is made more electrochemically reversible, the stability of ECL should be significantly improved. A similar argument has been made in considering the stability of electrochromic devices involving the generation of radical ions.[3]

In aprotic media, ECL involves light emission due to the electron transfer process in the vicinity of the electrode with the intensity largely governed by the stability of the electrogenerated radical ions over the time scale of the potential sweeps (or steps) and the quantum efficiency of the generated excited state.[1a] The ECL spectrum of a compound is usually the same as the fluorescence spectrum because both methods produce the same excited state. However, the ECL spectra of some PAHs, like pyrene, show another extra broad and structureless peak at longer wavelengths, which is attributed to the formation of excimer.[4] Long wavelength emission can also be attributed to the formation of a byproduct during the electrolysis, for example, by the decomposition of the radical cation, as seen in ECL of anthracene.[1e]

Fluorene-based molecules, like oligofluorenes[2a] and terfluorenes[5] are of interest in ECL and organic light emitting devices (OLED) because of their good electrochemical and thermal stabilities and high quantum yields. The present work reports that capping a DPA derivative, pyrene and anthracene, with two fluorene derivatives produces new aromatic hydrocarbons (**FDF**, **FPF**, **FAF**) (Figure 1) with very interesting ECL behavior, with enhanced ECL efficiency and stability as compared to their parent PAHs.

Figure 2 depicts a comparison of the cyclic voltammograms (CV) of **FAF**, **FDF**, and **FPF** and their parent counterparts. The electrochemical data are summarized in Table 1. **FAF** exhibits two oxidation peaks (Figure 2a). The first oxidation at $E^{\circ}_{1,ox} = 1.13$ V vs. SCE is reversible, at a less

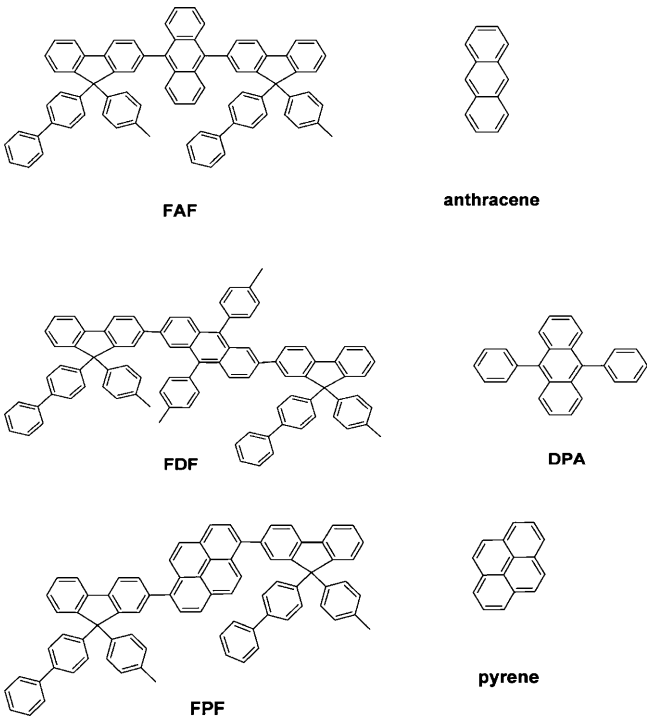

Figure 1. Chemical structures of the new ECL active aromatic compounds and model compounds.

[*] K. M. Omer, A. J. Bard
Center for Electrochemistry, Department of Chemistry and Biochemistry and Center for Nano- and Molecular Science and Technology, University of Texas at Austin
Austin, TX 78712 (USA)
E-mail: ajbard@mail.utexas.edu
S.-Y. Ku, K.-T. Wong
Department of Chemistry, National Taiwan University
106 Taipei (Taiwan)
E-mail: kenwong@ntu.edu.tw

[**] We thank Roche (BioVeris), The Robert A. Welch Foundation (F0021), the National Science Foundation NSF (CHE-0808927), and the National Science Council of Taiwan for supporting this work. We thank Shu-Hua Chou for her assistance with theoretical calculations.

Supporting information for this article is available on the WWW under http://dx.doi.org/10.1002/anie.200904156.

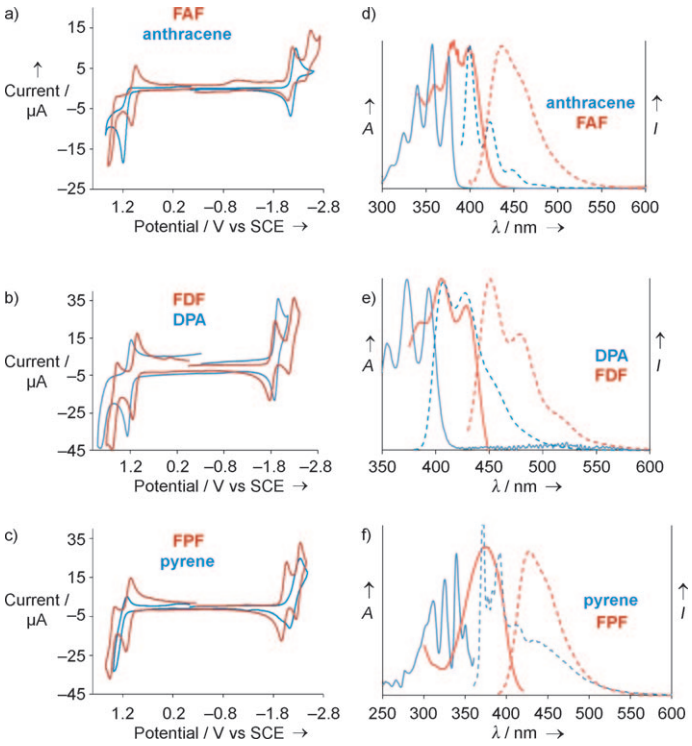

Figure 2. Cyclic voltammograms of a) **FAF** and anthracene, b) **FDF** and DPA, and c) **FPF** and pyrene. Conditions: 1 mM compound, 0.1 M Bu_4NPF_6 as supporting electrolyte in benzene/MeCN (1:1), scan rate 100 $mV s^{-1}$; working electrode: Pt disk (1 mm diameter), counter electrode: Pt wire, reference electrode: Ag wire (calibrated vs Fc/Fc^+). Normalized absorption (solid line) and emission spectra (dotted line, excited at absorption maxima) of d) **FAF** and anthracene, e) **FDF** and DPA, and f) **FPF** and pyrene in MeCN/benzene (1:1).

Table 1: Electrochemical data of **FAF**, **FDF**, and **FPF** as compared to their parent counterparts.[a]

	Oxid. [V]		Red. [V]		
Cmpd.	$E^\circ_{1,ox}$	$E^\circ_{1,ox}$	$E^\circ_{1,red}$	$E^\circ_{2,red}$	D [$cm^2 s^{-1}$]
FAF	1.13	1.57(E_p)	−1.92	−2.29	9.5×10^{-6}
anthracene	1.24(E_p)	–	−2.09	–	
FDF	1.05	1.48	−1.87	−2.27	9.0×10^{-6}
DPA	1.15	1.58(E_p)	−2.06	–	
FPF	1.10	1.43	−2.00	−2.30	9.0×10^{-6}
pyrene	1.16	–	−2.19	–	

[a] All potentials are versus SCE,* where $E^\circ(Fc/Fc^+) = 0.424$ V vs. SCE. D: diffusion coefficient.

positive potential than the parent anthracene by 130 mV (anthracene, $E_p = 1.24$ V; E_p is peak potential).[6] The second oxidation of **FAF** at $E_{p2,ox} = 1.57$ V is irreversible even with a scan rate of 2000 $mV s^{-1}$. As shown in Figure 2a, the oxidation of anthracene is totally irreversible. Aikens et al. suggested that the irreversible oxidation of anthracene can be attributed to the nucleophilic attack by solvent on the *meso* positions of anthracene leading to the decomposition of the radical cations.[7] Thus, C9 and C10 aryl-substituted anthracenes, such as DPA and **FAF**, can efficiently suppress the decomposition process, and allow reversible oxidations. The irreversible second oxidation of **FAF** indicates the dication FAF^{2+} is unstable, which we believe is due to the lack of additional substitutions on the C2 and C6 positions of anthracene. In addition, **FAF** shows two sequential reduction peaks at $E^\circ_{1,red} = -1.92$ V and $E^\circ_{2,red} = -2.29$ V vs. SCE, whereas anthracene exhibits only one higher reduction peak at $E^\circ_{1,red} = -2.09$ V. Although the electrochemical behavior of **FAF** is close to that of DPA, the second reduction of **FAF** is clearly seen while that of DPA could not be detected within the potential window of the solvent used in this experiment.

FDF, with C2, C6, C9, and C10 aryl-blocked anthracene core, reversibly oxidizes to give its first oxidation at $E^\circ_{1,ox} = 1.05$ V (for DPA, $E^\circ_{1,ox} = 1.15$ V)[8] and the second reversible oxidation peak at $E^\circ_{2,ox} = 1.48$ V (compared to DPA with an irreversible wave, even at higher scan rates, $E_{p2,ox} = 1.58$ V)(Figure 2b)). The observed peak separation for the reversible waves was ca. 80 mV, larger than expected peak splitting for ideal nernstian behavior, where a one-electron redox wave is expected to have a peak separation of ca. 59 mV. However, the internal standard, ferrocene, which is known to show nernstian behavior showed a similar peak separation under the same conditions. Thus, the observed peak separation can be attributed to ohmic drop ($\approx$1200 ohm) that is often observed with aprotic solvents. Scan rate studies (Supporting Information, Figure S1, S2) showed that the anodic and cathodic peak currents (i_{pa}, i_{pc}) of the first oxidation wave were proportional to the square root of scan rate ($\nu^{1/2}$) while the corresponding peak potentials (E_{pa}, E_{pc}) were independent of ν. Additionally, the peak current ratio (i_{pa}/i_{pc}) was approximately unity down to a scan rate of 100 $mV s^{-1}$, indicating the absence of a subsequent chemical reaction upon oxidation. **FDF** shows two reversible reduction peaks with each reduction peak height and separation ($\approx$80 mV) equal to those of the oxidation waves, indicating that each reduction is a one-electron transfer process. The potentials of the reduction waves were $E^\circ_{1,red} = -1.78$ V and $E^\circ_{2,red} = -2.27$ V, while for DPA, only one reduction at $E^\circ_{1,red} = -2.06$ V was detected. The lower first oxidation potential (by 100 mV) and reduction potential (by 280 mV) and the reversibility of the second oxidation and reduction processes indicate that radical ions and doubly charged moieties are more stable in **FDF** than in DPA. This can be attributed to the enhanced π-conjugation, rendering the delocalization of charges throughout the parent DPA core and fluorene substitutions, although the DFT calculation (B3LYP/STO-3G) on the energy-optimized molecular geometry of **FDF** (Figure S3) reveals the dihedral angles between the DPA core and two C9-biphenyl substituted fluorene rings are 29.4° and 31.5°, respectively. Thus, the introduction of fluorene peripherals on C2 and C6 of anthracene not only stabilizes the radical ions, but also blocks the active positions subject to decomposition, giving rise to extra stabilization on the highly charged species (dication and dianion).

As compared to pyrene (Figure 2c), **FPF** shows two oxidation waves $E^\circ_{1,ox} = 1.10$, $E^\circ_{2,ox} = 1.43$ V vs. SCE. The first oxidation is reversible at all scan rates ranging from 50 mV to 10 $V s^{-1}$, while the second oxidation shows reversibility only

with the scan rates beyond 250 mV s^{-1}. In addition, two sequential reversible reduction peaks ($E^{\circ}_{1,red} = -2.00$ V, $E^{\circ}_{2,red} = -2.30$ V vs. SCE), even at low scan rates, were detected. The lower potentials and reversibility of electron transfer processes as compared to those of pyrene agree with the stabilization effects of fluorene substitutions. The perturbation of the redox potentials, after capping with fluorenes, is more pronounced in **FDF** than in **FPF**, implying better electronic interactions between fluorenyl peripherals and DPA than in the case of pyrene. However, it is reasonable to anticipate that these new molecules should provide efficient ECL with higher stability due to the increase in lifetimes of the oppositely charged radicals, which subsequently annihilate to form the excited states.

Electronic absorption and photoluminescence (PL) spectra of **FAF**, **FDF**, and **FPF** are shown in Figure 2 d–f. The photophysical data are summarized in Table 2. All spectra of the new compounds show evident shifts to lower energy as compared to their parent compounds because of the increased π-conjugation in the new chromophores, agreeing with our observations in electrochemical studies. These new compounds generally show small Stokes shifts, which can be attributed to the structural rigidity and low

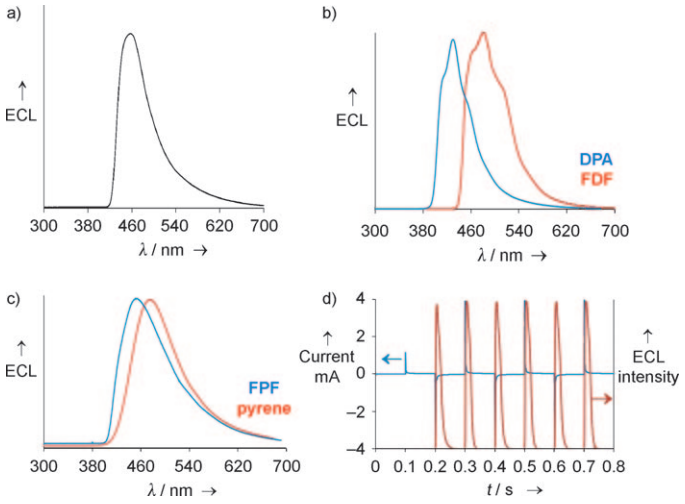

Figure 3. Normalized ECL spectra of a) **FAF**, b) DPA and **FDF**, c) pyrene and **FPF** taken in the same solution used for electrochemistry experiments shown in Figure 1. Pulsing is from $E_{p1,ox} = +80$ mV to $E_{p1,red} = -80$ mV with integration time of 10 s for each sample and a slit width of 0.5 mm. d) Transient ECL experiment, electrochemical current (blue line), ECL intensity (red line) for **FDF**. Pulse width: 0.1 s, sampling time: 1 ms, pulsing pattern: 0 V to negative ($E_{p1,red} = -80$ mV) to anodic ($E_{p1,ox} = +80$ mV).

Table 2: Photophysical properties of **FDF**, **FPF**, and **FAF** as compared to their parent compounds.[a]

Cmpd.	$\lambda_{max,Abs}$ [nm]	$\lambda_{max,PL}$ [nm]	Φ_{PL}	Stokes shift
FAF	341, 360, 380, 400	437	0.62	37
anthracene	310, 327, 340, 357, 376	400, 423, 450, 482		24
FDF	385, 407, 430	452, 485, 516(*sh*)	0.90	22
DPA	355, 373, 393	408, 429, 450(*sh*)		15
FPF	373	430	0.81	57
pyrene	311, 324, 340	392, 413, 440, 470(*ex*)		52

[a] Solvent is MeCN/benzene (1:1) for all the compounds. *sh*: shoulder, *ex*: excimer.

Table 3: Photophysical and ECL parameters of **FAF**, **FDF**, and **FPF**.

Cmpd.	$\lambda_{max,PL}$ [nm]	$\lambda_{max,ECL}$ [nm]	E_s[a]	$\Delta H°_{an}$[b]	Φ_{PL}	$\Phi_{r,ECL}$[c]
FAF	437	450	2.92	2.95	0.62	0.65
FDF	451, 482, 516(*sh*)	460, 485, 513(*sh*)	2.81	2.82	0.90	0.90
FPF	430	445	3.05	3.00	0.81	0.85

[a] E_s calculated based on $^1/_2(E_{absorption} + E_{emission})$. [b] $\Delta H_{an} = E^{\circ}_{1,ox} - E^{\circ}_{1,red} - 0.1$ eV. [c] $\Phi_{r,ECL}$ is the relative ECL compared to DPA, taking $\Phi^{ECL}_{DPA} = 1$. *sh*: shoulder.

polarity of the excited states.[10] The rigid structural features also contribute to the high efficiencies of PL, leading to high quantum yields of 0.62 for **FAF**, 0.90 for **FDF**, and 0.81 for **FPF**. As indicated in Figure 2 f, a broad tailing can be detected in the pyrene emission spectrum, which is ascribed to the excimer of pyrene formed in MeCN/Benzene (1:1). The red-shifted PL without excimer emission of **FPF** indicates the introduction of fluorene substitutions and not only increases the π-conjugation, but also imparts steric hindrance that prevents excimer formation.

Figure 3 depicts the ECL spectra of the highly efficient emitters **FAF**, **FDF**, and **FPF** compared with their parent compounds. The ECL results are summarized in Table 3. The high intensity allowed the ECL spectra of these new emitters to be taken with only a 10 s integration time; such strong emitters are very rare in ECL research. Typically, slight red shifts in the ECL spectra were observed as compared to their PL. This is attributed to the inner filter effect due to the difference in concentrations used for PL and ECL.

Anthracene shows poor ECL through direct annihilation reaction in aprotic solvents because of the irreversibility of oxidation (Figure 2 a).[12] Since the radical cation of anthracene has a very short life-time, a pulse width of 0.05 s and rigorous purification of DMF are required for the detection of anthracene ECL. In contrast, **FAF**, with fluorene protection on the C9 and C10 positions of anthracene, exhibits good electrochemical reversibility for both the oxidation and reduction processes, leading to very strong and stable bright blue ECL (450 nm) (Figure 3 a). The ECL spectrum of **FDF** compared to DPA is shown in Figure 3 b. **FDF** gives a maximum ECL emission peak at $\lambda^{ECL} = 485$ nm, which is red-shifted ca. 50 nm as compared to that of DPA. The ECL emission observed for **FDF** was almost as intense as that of DPA under the same conditions. They have similar fluorescence and ECL quantum yields ($\Phi^{PL}_{FDF} = 0.90$, $\Phi^{PL}_{DPA} = 0.91$, $\Phi^{ECL}_{FDF} \approx \Phi^{ECL}_{DPA}$). The question of long-term stability upon pulse cycling has always been of interest in ECL because of possible device applications.[13] Although the radical ions are apparently stable on the CV time scale, the ECL of DPA tends to decrease with extended pulsing. As shown in Figure 3 d, the transient ECL of **FDF** retains a constant intensity for each

pulse (pulsing from $E_{p1,ox}$ +80 mV to $E_{p1,red}$ −80 mV), indicating the ECL emission with **FDF** is more stable than DPA. The ECL of **FDF** was stable for at least 20000 pulses (0.1 s/pulse). These results are consistent with our observations that the second oxidation of DPA is not stable even with scan rates up to 1 $V s^{-1}$, while the second oxidation of **FDF** is stable even at a scan rate of 100 $mV s^{-1}$.

The ECL of pyrene from radical ion annihilation shows only excimer emission at $\lambda^{ECL} = 470$ nm.[4] Instead, **FPF** shows bright blue ECL ($\lambda^{ECL} = 445$ nm) without the indication of excimer formation during the electron transfer processes (Figure 3c). The steric hindrance of fluorene substitution in **FPF** prevents π-stacking for excimer formation during the electron transfer reaction, leading a high ECL quantum yield of 0.85 for **FPF**. By comparing the enthalpy of annihilation reaction, $\Delta H_{an} = E^{\circ}_{ox} - E^{\circ}_{red} - 0.1$ (in eV), to the energy required for excited state formation, E_s, as shown in Table 3, ECL for all three compounds follows the S-route, that is, availability of sufficient energy in the electron transfer reaction to populate to the singlet excited state directly.

In conclusion, fluorene was used as a capping agent to produce DPA, pyrene, and anthracene derivatives as new aromatic hydrocarbons (**FDF**, **FPF**, **FAF**). The introduction of fluorene groups imparts steric hindrance that prevents interchromophore interactions, giving these molecules high PL quantum yields. The fluorene substitutions also block the active positions of the PAH cores subject to electrochemical decomposition permitting the formation of stable radical ions and enhancing π-conjugation facilitating the charge delocalization. More importantly, the C2 and C6 substitutions on the DPA core provide extra stabilization for the highly charged species (dication and dianion), allowing **FDF** to have highly efficient ($\Phi^{ECL}_{FDF} = 0.90$) and stable (up to 20000 pulses) blue ECL. The calculated enthalpies of these annihilation reactions indicate that the electron transfer reactions for ECL follow an S-route.

Received: July 27, 2009
Revised: September 25, 2009
Published online: November 4, 2009

Keywords: electrochemistry · electrogenerated chemiluminescence · oligofluorene · polyaromatic hydrocarbon

[1] a) *Electrogenerated Chemiluminescence* (Ed.: A. J. Bard), Marcel Dekker, New York, **2004**; b) D. M. Hercules, *Science* **1964**, *145*, 808–809; c) R. E. Visco, E. A. Chandross, *J. Am. Chem. Soc.* **1964**, *86*, 5350–5351; d) K. S. V. Santhanam, A. J. Bard, *J. Am. Chem. Soc.* **1965**, *87*, 139–140; e) L. R. Faulkner, A. J. Bard, *J. Am. Chem. Soc.* **1968**, *90*, 6284–6290.

[2] a) M. M. Sartin, C. Shu, A. J. Bard, *J. Am. Chem. Soc.* **2008**, *130*, 5354–5360; b) M. M. Sartin, H. Zhang, J. Zhang, P. Zhang, W. Tian, Y. Wang, A. J. Bard, *J. Phys. Chem. C* **2007**, *111*, 16345–16350; c) K. M. Omer, A. L. Kanibolotosky, P. J. Skabara, I. F. Perepichka, A. J. Bard, *J. Phys. Chem. B* **2007**, *111*, 6612–6619.

[3] H. J. Byker, US Patent, 4,902,108 (February 20, **1990**).

[4] a) E. A. Chandross, J. W. Longworth, R. E. Visco, *J. Am. Chem. Soc.* **1965**, *87*, 3259–3260; b) D. M. Hercules, J. Chang, T. C. Werner, *J. Am. Chem. Soc.* **1970**, *92*, 5560–5565; c) J. T. Maloy, A. J. Bard, *J. Am. Chem. Soc.* **1971**, *93*, 5968–5981; d) B. Fleet, G. F. Kirkbright, C. J. Pickford, *J. Electroanal. Chem.* **1971**, *30*, 115–121; e) T. Kihara, M. Sukigara, K. Honda, *J. Electroanal. Chem.* **1973**, *47*, 161–166; f) C. P. Keszthelyi, A. J. Bard, *Chem. Phys. Lett.* **1974**, *24*, 300–304; g) H. Tachikawa, A. J. Bard, *Chem. Phys. Lett.* **1974**, *26*, 568–573; h) T. Suminaga, S. Hayakawa, *Bull. Chem. Soc. Jpn.* **1980**, *53*, 315–318.

[5] OLEDs: a) K.-T. Wong, R.-T. Chen, F.-C. Fang, C.-C. Wu, Y.-T. Lin, *Org. Lett.* **2005**, *7*, 1979–1982; b) Y. Geng, D. Katsis, S. W. Culligan, J. J. Ou, S. H. Chen, L. J. Rothberg, *Chem. Mater.* **2002**, *14*, 463–470; c) K.-T. Wong, Y.-Y. Chien, R.-T. Chen, C.-F. Wang, Y.-T. Lin, H.-H. Chiang, P.-Y. Hsieh, C.-C. Wu, C. H. Chou, Y. O. Su, G.-H. Lee, S.-M. Peng, *J. Am. Chem. Soc.* **2002**, *124*, 11576–11577.

[6] C. K. Mann, K. K. Barnes, *Electrochemical Reactions in Nonaqueous Systems*, Marcel Dekker, New York, **1970**.

[7] a) A. E. Coleman, H. H. Richtol, D. A. Aikens, *J. Electroanal. Chem.* **1968**, *18*, 165–174; b) T. C. Werner, J. Chang, D. M. Hercules, *J. Am. Chem. Soc.* **1970**, *92*, 763–768.

[8] M. M. Sartin, C. Shu, A. J. Bard, *J. Am. Chem. Soc.* **2008**, *130*, 5354–5360.

[9] R. Andruzzi, A. Trazza. L. Greci, L. Marchetti, *J. Electroanal. Chem.* **1980**, *108*, 49–58.

[10] C. Reichardt, *Solvents and Solvent Effects in Organic Chemistry*, Wiley, New York, **2003**.

[11] S. A. Cruser, A. J. Bard, *J. Am. Chem. Soc.* **1969**, *91*, 267–275.

[12] D. Laser, A. J. Bard, *J. Electrochem. Soc.* **1975**, *122*, 632–640.

[13] a) L. R. Faulkner, A. J. Bard, *J. Am. Chem. Soc.* **1968**, *90*, 6284–6290; b) L. R. Faulkner, A. J. Bard, *J. Am. Chem. Soc.* **1969**, *91*, 209–210.

